

# PW based phase change nanocomposites containing $\gamma\text{-Al}_2\text{O}_3$

Jifen Wang · Huaqing Xie · Yang Li ·  
Zhong Xin

Received: 7 November 2009 / Accepted: 26 April 2010 / Published online: 18 May 2010  
© Akadémiai Kiadó, Budapest, Hungary 2010

**Abstract** Phase change nanocomposites were prepared by dispersing  $\gamma\text{-Al}_2\text{O}_3$  nanoparticles into melting paraffin wax (PW). Intensive sonication was used to make well dispersed and homogeneous composites. Differential scanning calorimetric (DSC) and transient short-hot-wire (SHW) method were employed to measure the thermal properties of the composites. The composites decreased the latent heat thermal energy storage capacity,  $L_s$ , and melting point,  $T_m$ , compared with those of the PW. Interestingly, the composites with low mass fraction of the nanoparticles, have higher latent heat capacity than the calculated latent heat capacity value. The thermal conductivity of the nanocomposites was enhanced and increased with the mass fraction of  $\text{Al}_2\text{O}_3$  in both liquid state and solid state.

**Keywords** Phase change composites · Thermal properties · Paraffin wax ·  $\gamma\text{-Al}_2\text{O}_3$

## Introduction

Paraffin wax (PW) with low melting temperature ( $T_m$ ), high latent heat capacity ( $L_s$ ) and small temperature variation from storage to retrieval is often used as phase change material (PCM) [1–5]. However, the low thermal conductivity as the major drawback limits its utility areas. It leads to decreasing

the rates of heat storage and retrieval during melting and solidification processes. To overcome the problem of low thermal conductivity, a wide range of investigations were carried out to enhance the thermal conductivity of PW [6, 7]. Aluminum and other metallic particles have been extensively used in energy-conversion applications due to their unusual energetic properties. Several studies proved that a small amount of metal or nonmetal nanoparticles could greatly increase the thermal conductivity of the based fluids or condense materials [8, 9]. In the past decade, nanofluids become one of the most attractive heat transfer media.  $\text{Al}_2\text{O}_3$  nanoparticles were often used as additives in nanofluids because of the high thermal conductivity and cheap price among the metal oxide nanoparticles. Nanofluids containing  $\text{Al}_2\text{O}_3$  in water were reported to have higher heat transfer enhancement than those containing  $\text{CuO}$  with same volume fraction [9, 10]. However, there is no significant theoretical or experimental study that deals with the addition of the  $\text{Al}_2\text{O}_3$  nanoparticles on the thermal transport of the composites as PCMs.

In this paper, we present the investigation on a novel thermal performance enhanced PCM.  $\text{Al}_2\text{O}_3$  nanoparticles are used as additives for tailoring the thermal properties of the matrix material, PW. Oleylamine is employed to treat the nanoparticles with poor dispersibility. The thermal conductivity of the prepared PCM nanocomposites is investigated and the mechanism of the thermal transport enhancement is further discussed.

J. Wang · Z. Xin  
State Key Laboratory of Chemical Engineering, East China  
University of Science and Technology, Shanghai 200237, China

J. Wang · H. Xie (✉) · Y. Li  
School of Urban Development and Environmental Engineering,  
Shanghai Second Polytechnic University, Shanghai 201209,  
China  
e-mail: hqxie@eed.sspu.cn

## Experimental

### Preparation of the nanocomposites

PW (industrial grade) with melting temperature of 325–327 K was obtained from Sinopharm Chemical

Reagent Co. Ltd. The PW was used without further purification.  $\text{Al}_2\text{O}_3$  nanoparticles (99.9%) are obtained from Hangzhou Jingtian Nanotech. Co. Ltd. The density of the  $\text{Al}_2\text{O}_3$  nanoparticles is  $3.9 \text{ g/cm}^3$ . The average diameter of the particles is about 20 nm.

The  $\text{Al}_2\text{O}_3$  powders were added into melting PW in a mixing container. Oleylamine was already dispersed in the PW. The mixture was subjected to intensive sonication to make well dispersed and homogeneous PW/ $\text{Al}_2\text{O}_3$  composites.  $\text{Al}_2\text{O}_3$  nanoparticles with mass fractions of 1–5 wt% were dispersed in PW to prepare the composites.

### Characterization

Various analytical methods have been applied to characterize the  $\text{Al}_2\text{O}_3$  nanoparticles. Transmission electron microscopy (TEM) pictures were taken on a JEOL 2100F high resolution TEM device. Scanning electron microscopy (SEM) observation was performed on a Hitachi S-4800 field emission SEM device. Fourier transformation infrared (FTIR) spectra were collected on a Bomem DA 8 spectrometer. X-ray diffraction (XRD) patterns were recorded on a D8-Advance diffractometer using Cu K $\alpha$  X-ray at 40 kV and 100 mA.

Thermal properties including melting temperature ( $T_m$ ) and latent heat capacity ( $L_s$ ) of pure PW and PW/ $\text{Al}_2\text{O}_3$  composites were measured using a differential scanning calorimetric (DSC) instrument (Diamond DSC, Perkin Elmer, USA). The DSC measurements were performed at a heating rate of  $5 \text{ K min}^{-1}$  and in a temperature range of 273–348 K.

Thermal conductivities ( $k$ ) of the pure PW and the PW/ $\text{Al}_2\text{O}_3$  composites were measured by a transient short-hot-wire (SHW) method. The detailed measurement principle and procedure have been described elsewhere [11–13]. Briefly a platinum wire with a diameter of 70  $\mu\text{m}$  was used for the hot wire, and it served as both a heating unit and as an electrical resistance thermometer. Initially the platinum wire immersed in media was kept at equilibrium with the surroundings. The uncertainty of this measurement is estimated to be less than  $\pm 1.0\%$ . For thermal conductivity measurements, the PCM sample was melted and poured into a stainless steel cylinder container. A platinum wire and a thermocouple were immersed in the PCM to record and test the temperature of the PCM before a waterproof lid covered the container. The container was put into a water bath with a temperature of 288 K. When the thermocouple in the PCM showed the temperature vibration less than 0.1 K for 10 min it was taken for the hot wire probe in an isotropic medium. The hot wire probe was subjected at time  $t = 0$  to a step change in the electrical current applied to the wire. The temperature of the water bath was increased every 10 K from 288 to 318 K while increased

every 5 K from 328 to 338 K. At every temperature, three measurements were conducted and the average value was taken as the result.

## Results and discussion

### Analysis of the $\text{Al}_2\text{O}_3$ nanoparticles

The SEM and TEM images of the used  $\text{Al}_2\text{O}_3$  nanoparticles were shown in Fig. 1. In these figures, the  $\text{Al}_2\text{O}_3$  nanoparticles are turned to be spherical and club-shaped. The diameter of the particles is fairly uniform and the average diameter of the particles is 20 nm. Figure 2 presents the FTIR spectrum of  $\text{Al}_2\text{O}_3$  nanoparticles. In Fig. 2, there is transmission band centered at about  $3400 \text{ cm}^{-1}$ , characteristic of hydrogen bonded –O–H of the adsorbed water. The band at  $1384 \text{ cm}^{-1}$  is corresponding to the phonon lengthways stretching band of  $\text{Al}_2\text{O}_3$  [14, 15], while the band at  $500$ – $1000 \text{ cm}^{-1}$  can be interpreted to be the bending stretching band of Al–O [16]. The transmission band at  $1639 \text{ cm}^{-1}$  is the characteristic of the bending stretching of the adsorbed  $\text{H}_2\text{O}$ , while the bands at  $2852$  and  $2923 \text{ cm}^{-1}$  are the characteristics of the adsorbed  $\text{CO}_2$ . Figure 3 shows the XRD pattern of the  $\text{Al}_2\text{O}_3$  nanoparticles. The broad bands at  $30^\circ$ – $40^\circ$  and strong bands at  $46^\circ$  and  $67^\circ$  mean that the structure of the sample is  $\gamma$ -phase.

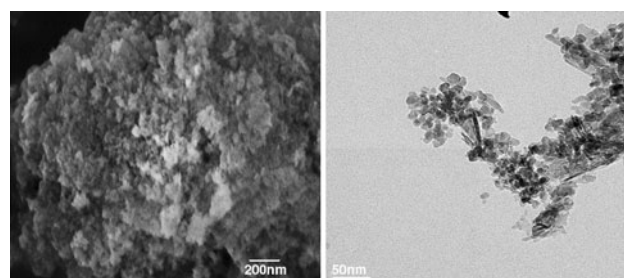


**Fig. 1** SEM (left) and TEM (right) image of  $\text{Al}_2\text{O}_3$  particles

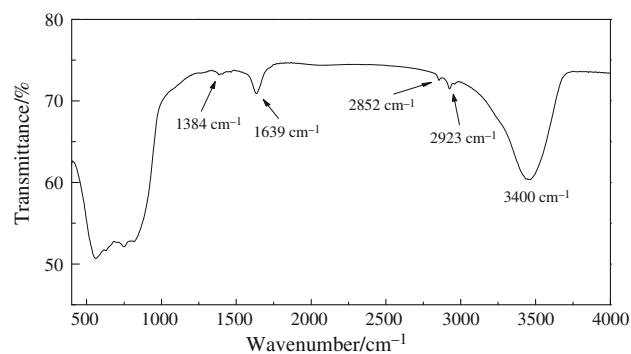


**Fig. 2** FTIR spectrum of  $\text{Al}_2\text{O}_3$  nanoparticles

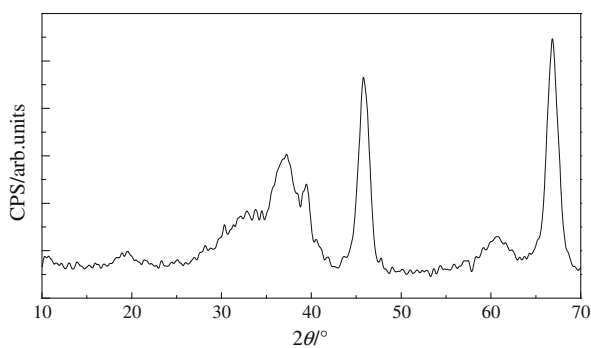


**Fig. 3** XRD pattern of Al<sub>2</sub>O<sub>3</sub> nanoparticles

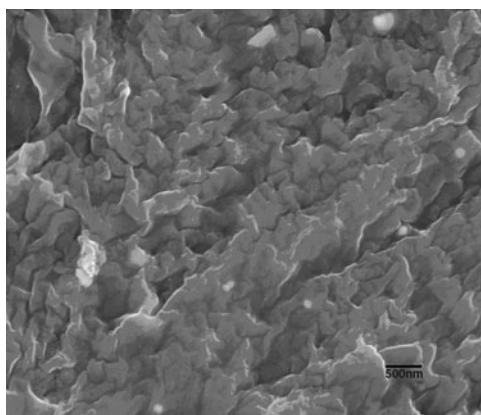


**Fig. 4** SEM image of the composite with Al<sub>2</sub>O<sub>3</sub> mass fraction of 5%

#### Compatibility of the composites

In order to see how the dispersity of the Al<sub>2</sub>O<sub>3</sub> particles in the PW matrix, the SEM image of the composite was given in Fig. 4. The mass fraction of the selected sample is 5%. It is observed that the composite is homogeneous and the Al<sub>2</sub>O<sub>3</sub> particles are separated individually in PW.

#### Melting temperature and latent heat capacity

The phase change temperature and latent heat capacity of the PW and the composites were measured to investigate the influence of the Al<sub>2</sub>O<sub>3</sub> nanoparticles addition on the thermal properties of the composites. Table 1 presents the result of the DSC analysis including the solid–solid phase

change temperature ( $T_{s-s}$ ), melting temperature ( $T_m$ ), latent heat capacity of solid–solid phase change ( $L_{s-s}$ ) and of solid–liquid phase change ( $L_s$ ). The data of calculated latent heat capacity (Cal.  $L_{s-s}$  and Cal.  $L_s$ ) are obtained by multiplying the value of the latent heat capacity ( $L_{s-s}$  and  $L_s$ ) of the pure PW with the mass ratio of the PW in the composites. It is seen from Table 1 that the phase change temperature both  $T_{s-s}$  and  $T_m$  shift to a lower temperature due to the addition of Al<sub>2</sub>O<sub>3</sub> into PW, except the composite with Al<sub>2</sub>O<sub>3</sub> mass fraction of 1%. All the composites decrease the latent heat capacity  $L_s$ , compared with the PW. The composite with Al<sub>2</sub>O<sub>3</sub> mass fraction of 1% increases  $L_{s-s}$  by 2.2 J g<sup>-1</sup>, compared with pure PW. Interestingly, the data of  $L_{s-s}$  for the composites, with Al<sub>2</sub>O<sub>3</sub> mass fraction of 1 and 2%, are higher than the Cal.  $L_{s-s}$  by 2.5 and 0.3 J g<sup>-1</sup> while the composite with Al<sub>2</sub>O<sub>3</sub> mass fraction of 5% is lower than the Cal.  $L_{s-s}$ . The data of  $L_s$  of all the composites are lower than that of the PW and their Cal.  $L_s$ . This might be caused by the interaction between the PW molecules and the Al<sub>2</sub>O<sub>3</sub> particles [17]. The PW increases its volume with the increasing of the temperature, that is, the matrix structure of the PW turns expanded when temperature rising. However, the interactions between the PW molecules and the Al<sub>2</sub>O<sub>3</sub> particles are stronger than those between the PW molecules at  $T_{s-s}$  but weaker at  $T_m$ .

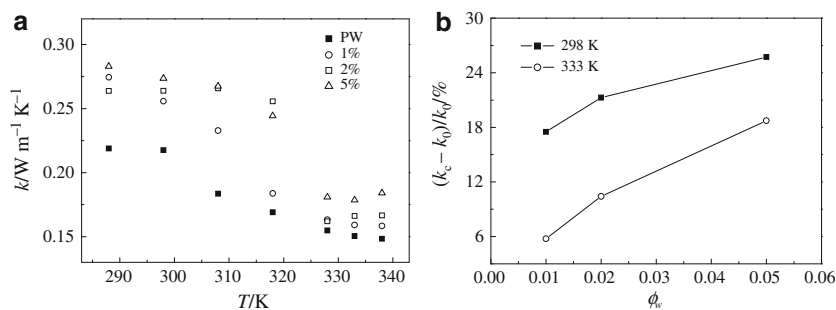
#### Thermal conductivity improvement

Thermal conductivity is one of the most important properties of PCMs. Thermal conductivity enhancement is expected in the composites with Al<sub>2</sub>O<sub>3</sub> particles addition since Al<sub>2</sub>O<sub>3</sub> have high thermal conductivity. To investigate the effect of Al<sub>2</sub>O<sub>3</sub> particles on the thermal conductivity of phase change composites containing Al<sub>2</sub>O<sub>3</sub>, PW based composites at different Al<sub>2</sub>O<sub>3</sub> loadings were prepared and their thermal conductivities were measured by the SHW method. Figure 5a shows the temperature dependent thermal conductivity of the PW and the composites. The thermal conductivities of the composites are higher than those of the PW at the same temperature. Interestingly, the thermal conductivities of the PW and the composites decrease with an increase in the temperature at the solid state. The thermal conductivities of the composites increase with the Al<sub>2</sub>O<sub>3</sub> particles in the composites in the

**Table 1** The phase change temperature and latent heat capacity of PCMs

PCMs	$T_{s-s}/\text{K}$	$T_m/\text{K}$	$L_{s-s}/\text{J g}^{-1}$	$L_s/\text{J g}^{-1}$	Cal. $L_{s-s}/\text{J g}^{-1}$	Cal. $L_s/\text{J g}^{-1}$
PW	303.2	321.2	31.4	142.2		
With 1% Al <sub>2</sub> O <sub>3</sub>	302.4	321.3	33.6	136.1	31.1	140.8
With 2% Al <sub>2</sub> O <sub>3</sub>	302.6	321.0	31.0	136.3	30.7	139.4
With 5% Al <sub>2</sub> O <sub>3</sub>	299.9	319.3	29.2	134.1	29.8	135.1

**Fig. 5** Temperature dependent  $k$  (a) and  $k$  enhancement as a function of  $\text{Al}_2\text{O}_3$  (b) of PCMs



solid state at the same temperature except for the composite with 2%  $\text{Al}_2\text{O}_3$  particles at 318 K higher than that with 5%  $\text{Al}_2\text{O}_3$  particles and 288 K lower than that with 1%  $\text{Al}_2\text{O}_3$  particles. The highest thermal conductivity of the composites is  $0.28 \text{ W m}^{-1} \text{ K}^{-1}$  of the composite with 5%  $\text{Al}_2\text{O}_3$  particles at 288 K in the solid state and  $0.19 \text{ W m}^{-1} \text{ K}^{-1}$  in the liquid state. The thermal conductivity of the composite with  $\text{Al}_2\text{O}_3$  mass fraction of 5% is higher than PW by about  $0.07 \text{ W m}^{-1} \text{ K}^{-1}$  in the solid state at 288 K and  $0.05 \text{ W m}^{-1} \text{ K}^{-1}$  in the liquid state at 338 K, respectively. We calculated the thermal conductivity enhancement ratios of the PW/ $\text{Al}_2\text{O}_3$  composites in order to show clearly the effect for the thermal transfer with adding  $\text{Al}_2\text{O}_3$  particles to PW. Figure 5b shows the thermal conductivity enhancements as functions of  $\text{Al}_2\text{O}_3$  mass fraction of the nanocomposites at 298 and 333 K.  $k_c$  and  $k_0$  represent the thermal conductivities of composites and pure PW, respectively.  $(k_c - k_0)/k_0$  is the thermal conductivity enhancement ratio of the nanocomposites. It is shown in the figure, thermal conductivity enhancement of the nanocomposite increases with an increase of  $\text{Al}_2\text{O}_3$  mass fraction at both 298 and 333 K. At 298 K, the slope of the line through the point  $\text{Al}_2\text{O}_3$  mass fraction of 1 and 2% is larger than that through 2 and 5%, as well as at 333 K. This indicates that there is not a simple relationship between the thermal conductivity enhancement and the mass fraction of the additives in the PW/ $\text{Al}_2\text{O}_3$  composites.

It is very complicated that how the factors would influence the composite on the thermal conductivity. The contributions of the thermal conductivity enhancement of a composite include the thermal conductivity of materials in the composite and the interaction between them. Thermal conductivity enhancement was expected for composite containing nanoparticles with high thermal conductivity. However, our experimental results indicated that the enhancement ratios of the thermal conductivity of the composite are much lower than the value predicted by effective medium theory [18]. This disappointing thermal performance can be attributed to two main reasons. One is the lower intrinsic matrix conductivity after treatment, possibly due to scattering of heat carrying phonons by interactions with the surroundings or from defects. The other is the thermal contact resistance at

the nanoparticle surfaces [19, 20]. Fu and Mai [21] reported the thermal conductivity of the composites increased almost linearly with carbon fiber content. When the additive thermal conductivity is high, the composite thermal conductivity increases significantly with the increase of mean fiber aspect ratio. While the fiber thermal conductivity is low, the composite thermal conductivity increases slowly with the increase of the additive ratio. As particulate composite, the  $\text{Al}_2\text{O}_3$  particles in the organic matrix can be regarded as a special case of short fiber composites with short fibers a low aspect ratio and random orientation.

## Conclusions

We prepared a series of stable, homogeneous, and thermal performance enhanced heat storage nanocomposite PCMs consisting of PW and  $\gamma$ - $\text{Al}_2\text{O}_3$  nanoparticles. DSC analysis revealed that the PW/ $\text{Al}_2\text{O}_3$  composites have reduced both melting point and latent heat capacity with an increase in the mass fraction of  $\text{Al}_2\text{O}_3$  nanoparticles. Due to the interaction of the  $\text{Al}_2\text{O}_3$  nanoparticles and the PW molecules during phase change process, the composites with low mass fraction of the nanoparticles have higher latent heat capacity compared to the calculated value. PW/ $\text{Al}_2\text{O}_3$  composites have enhanced thermal conductivities compared to the pure PW, with the enhancement ratios increasing with the mass fraction of  $\text{Al}_2\text{O}_3$  nanoparticles.

**Acknowledgements** This work was supported by National Science Foundation of China (50876058, 20876042), New Century Excellent Talents in University (NCET-10-883), and the Program for Professor of Special Appointment (Eastern Scholar) at Shanghai Institutions of Higher Learning.

## References

- Sari A, Alkan C, Karaipekli A, Önal A. Preparation, characterization and thermal properties of styrene maleic anhydride copolymer (SMA)/fatty acid composites as form stable phase change materials. Energy Convers Manage. 2008;49:373–80.
- Wang J, Xie H, Xin Z. Thermal properties of paraffin based composites containing multi-walled carbon nanotubes. Thermo-chim Acta. 2009;488:39–42.

3. Sari A, Karaipekli A. Preparation and thermal properties of capric acid/palmitic acid eutectic mixture as a phase change energy storage material. *Mater Lett.* 2008;62:903–6.
4. Dimaano MNR, Watanabe T. Performance investigation of the capric and lauric acid mixture as latent heat energy storage for a cooling system. *Sol Energy.* 2002;72:205–15.
5. Sari A. Thermal characteristics of a eutectic mixture of myristic and palmitic acids as phase change material for heating applications. *Appl Therm Energy.* 2003;23:1005–17.
6. Karaipekli A, Sari A, Kaygusuz K. Thermal conductivity improvement of stearic acid using expanded graphite and carbon fiber for energy storage applications. *Renew Energy.* 2007;32: 2201–10.
7. Fukai J, Kanou M, Kodama Y, Miyatake O. Thermal conductivity enhancement of energy storage media using carbon fibers. *Energy Convers Manage.* 2000;41:1543–56.
8. Lee J, Mudawar I. Assessment of the effectiveness of nanofluids for single-phase and two-phase heat transfer in micro-channels. *Int J Heat Mass Transf.* 2007;50:452–63.
9. Kim J-K, Jung JY, Kang YT. The effect of nano-particles on the bubble absorption performance, in a binary nanofluid. *Int J Refrig.* 2006;29:22–9.
10. Heris SZ, Etemad SG, Esfahany MN. Experimental investigation of oxide nanofluids laminar flow convective heat transfer. *Int Commun Heat Mass Transf.* 2006;33:529–35.
11. Sari A, Karaipekli A. Thermal conductivity and latent heat thermal energy storage characteristics of paraffin/expanded graphite composite as phase change material. *Appl Therm Energy.* 2007;27:1271–7.
12. Xie H, Gu H, Fujii M, Zhang X. Short hot wire technique for measuring thermal conductivity and thermal diffusivity of various materials. *Meas Sci Technol.* 2006;17:208–14.
13. Wang J, Xie H, Xin Z. Thermal properties of heat storage composites containing multi-walled carbon nanotubes. *J Appl Phys.* 2008;104(113537):1–5.
14. Ye X, Sha J, Jiao Z, et al. Size effect on structure and infrared behavior in nanocrystalline magnesium oxide. *Nano-Struct Mater.* 1997;8(7):945–51.
15. Zheng C, Zhang X, Zhang J, Liao K. Preparation and characterization of VO<sub>2</sub> nanopowders. *J Solid State Chem.* 2001;156:274–80.
16. Wang Y, Suryanarayana C, An L. Phase transformation in nanometer-sized  $\gamma$ -Al<sub>2</sub>O<sub>3</sub> by mechanical milling. *J Am Ceram Soc.* 2005;3:780–3.
17. Kumar DH, Patel HE, Kumar VRR, Sundararajan T, Pradeep T, Das SK. Model for heat conduction in nanofluids. *Phys Rev Lett* 2004;93(14):144301,1–4.
18. Huxtable ST, Cahill DG, Shenogin S, Xue L, Ozisik R, Barone P, et al. Effect of chemical functionalization on thermal transport of carbon nanotube composites. *Nat Mater.* 2003;2:731–4.
19. Papanikolaou N. Nonequilibrium radiation dosimetry. *J Phys Condens Matter.* 2008;20(135201):1–6.
20. Zhong HL, Lukes JR. Interfacial thermal resistance between carbon nanotubes: molecular dynamics simulations and analytical thermal modeling. *Phys Rev B.* 2006;74(125403):1–10.
21. Fu S-Y, Mai Y-W. Thermal conductivity of misaligned short-fiber-reinforced polymer composites. *J Appl Poly Sci.* 2003;88: 1497–505.